

Chapter 2

Concepts of Fracture Mechanics

Abstract To begin with, linear elastic behaviour is assumed to explicate the basic concepts of fracture mechanics, namely energy and stress intensity approaches. The respective terminology is introduced and the physical quantities of energy release rate and stress intensity factor are defined. Criteria for unstable “brittle” fracture based on the energy release rate and the stress intensity factor are established. Some analytical expressions for stress intensity factors of real structures are given and the problem of a cracked cylinder under internal pressure is addressed, in particular.

Classical fracture mechanics is based on the theory of continuum mechanics and constitutive equations for stable material behaviour (see Sect. 6.1.1 on stability postulates) like elasticity, plasticity or viscoplasticity. It does not account for any damage of the material preceding crack growth or any kind of material separation. It postulates the existence of a defect or crack in a body or structure and either analyses stress and strain fields at the “crack tip”, which is a singular point, or considers the energy balance of cracked and uncracked media to derive “crack driving forces” and respective criteria of crack extension. For actually modelling crack growth, the topology of the body has to be modified.

Generally, two basic concepts of classical fracture mechanics have been established, the energy and the stress intensity approach, which are outlined in the following for linear-elastic material behaviour, first, and extended to elasto-plasticity later (see Chap. 5 on elastic-plastic fracture mechanics).

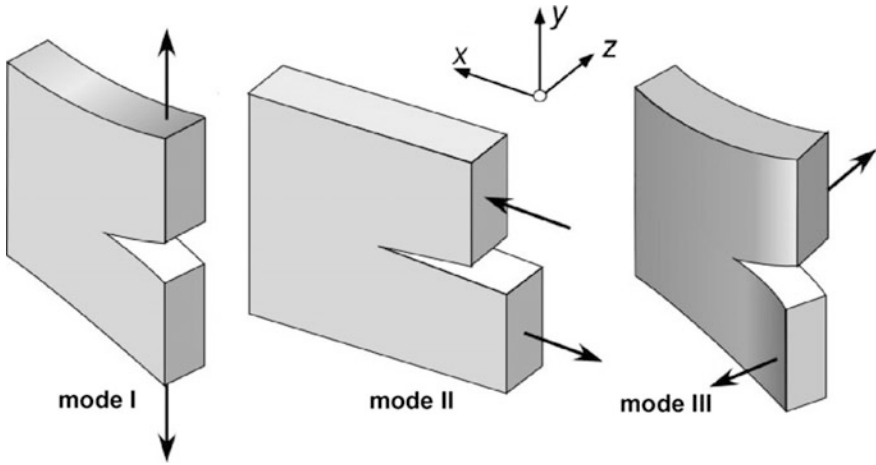
Linear-elastic fracture mechanics (LEFM) is based on Hooke’s equation postulating a linear relationship between stresses, σ_{ij} , and strains, ε_{ij} ,

$$\varepsilon_{ij} = \frac{1}{E} [(1 + \nu)\sigma_{ij} - \nu\sigma_{kk}\delta_{ij}] \quad (2.1)$$

with E being Young’s modulus and ν Poisson’s ratio, under the assumption of small deformations. The latter is actually not consistent with strain singularities occurring at a crack tip but it is essential for closed form solutions which represent a model of the conditions governing the physical state in some process zone of material degradation where the requirements of continuum mechanics are not met, anyway.

Table 2.1 Fundamental modes of crack displacements

Mode	Local appearance	Types of loading
Mode I	Opening of crack faces under tensile stresses normal to the crack plane	Loading by normal forces or bending, wedging of crack faces
Mode II	Slipping of crack faces along ligament	Pure shear forces, Inclined crack by 45° under biaxial tension-compression forces, Cutting and stamping processes
Mode III	Out-of-plane shearing	Torsion, anti-plane tearing

**Fig. 2.1** Fundamental modes of crack displacements according to Irwin [17]

Aside from inner circular (penny shaped) or elliptical cracks investigated by Sneddon [35] and Irwin [18], respectively, most analytical models of cracked bodies are two-dimensional. They represent panels of arbitrary in-plane shape but constant thickness, B , with through-thickness cracks. Irwin [17] identified three fundamental modes of crack displacements, Table 2.1 and Fig. 2.1. Loading in mode I and mode II is in-plane, and in mode III is out-of-plane. Mode I configurations are particularly important in engineering practice (pressure vessels, bending of beams) and hence most frequently investigated.

The out-of-plane boundary conditions for panels in mode I or II is either plane strain (zero lateral strain, $\varepsilon_{zz} = 0$) or plane stress (zero lateral stress, $\sigma_{zz} = 0$), respectively, which are the limiting cases for very thick or very thin panels. The out-of-plane condition affects the in-plane deformation owing to Poisson's ratio, ν , which is captured by a modified Young's modulus,

$$E' = \begin{cases} \frac{E}{1-\nu^2} & \text{for plane strain, } \varepsilon_{zz} = 0 \\ E & \text{for plane stress, } \sigma_{zz} = 0 \end{cases} \quad (2.2)$$

and a factor κ , defined as

$$\kappa = \begin{cases} 3 - 4\nu & \text{for plane strain, } \varepsilon_{zz} = 0 \\ \frac{3-\nu}{1+\nu} & \text{for plane stress, } \sigma_{zz} = 0 \end{cases} \quad (2.3)$$

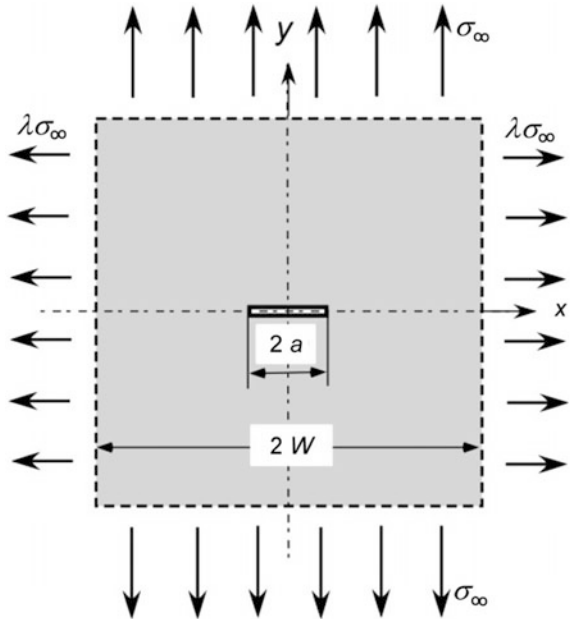
Extensions to “real” three-dimensional configurations will be addressed as required.

2.1 The Energy Approach of Griffith

The first one ever studying a cracked structure as an engineering problem was Griffith [11, 12], who treated the occurrence of fracture by the theorem of minimum energy and applied this theory to an “infinite” panel with a centre crack of length $2a$ under biaxial tension, see Fig. 2.2, where “infinite” indicates that the panel width, $2W$, is very large compared to the crack size, $a/W \ll 1$. This configuration is known as Griffith crack, since.

The elastic strain energy which is stored in a circular region of radius W of a panel without a crack is

Fig. 2.2 The Griffith crack: centre crack of length $2a$ in an “infinite” panel ($W \gg a$) under biaxial tension



$$U_0^e = \frac{\pi B W^2 \sigma_\infty^2}{16G} \left[(\kappa - 1)(1 + \lambda)^2 + 2(1 - \lambda)^2 \right], \quad (2.4)$$

where B is the panel thickness, σ_∞ the applied uniform far-field stress, $G = E/2(1 + \nu)$ the shear modulus and λ the biaxiality factor.

The strain energy depends on the size of the panel and becomes infinite for $W \rightarrow \infty$. If a hole is cut into the panel, stress and strain fields change and so does the strain energy. It increases or decreases depending on the boundary conditions. Assuming a constant far-field displacement, that is fixed grip, energy is released,

$$U^e = U_0^e - U_{\text{rel}}^e. \quad (2.5)$$

The decrease of strain energy due to an elliptical hole with principal axes $2a$ and $2c$ can be calculated with the equations of Inglis [16] as

$$U_{\text{rel}}^e = \frac{\pi B \sigma_\infty^2}{32G} (1 + \kappa) \left[(1 - \lambda)^2 (a + c)^2 + 2(1 - \lambda^2)(a^2 - c^2) + (1 + \lambda)^2 (a^2 + c^2) \right]. \quad (2.6)$$

It depends only on the dimensions of the hole and is always finite. The Griffith crack of length $2a$ is obtained for $c \rightarrow 0$,

$$U_{\text{rel}}^e = \frac{\pi a^2 B \sigma_\infty^2}{8G} (1 + \kappa). \quad (2.7)$$

Stresses $\lambda \sigma_\infty$ parallel to the crack do not affect the released energy.

Now Griffith established a condition for the crack to grow, which balances the released energy and the material resistance to crack extension,

$$\frac{\partial}{\partial (2a)} (U_{\text{rel}}^e - U_{\text{sep}}) \geq 0. \quad (2.8)$$

Note that the Griffith crack has a length of $2a$ with two crack tips. The second term, U_{sep} , the work of separation, equals the surface energy per unit thickness of the four crack faces,

$$U_{\text{sep}} = 4Ba\gamma. \quad (2.9)$$

Griffith [11] offered the following argument for his quite unconventional idea of the specific surface energy, γ : “Just as in a liquid, so in a solid the bounding surfaces possess a surface tension which implies the existence of a corresponding amount of potential energy. If owing to the action of a stress a crack is formed, or a pre-existing crack is caused to extend, therefore, a quantity of energy proportional to the area of the new surface must be added”.

An existing crack will start to extend in an unstable manner if the equality sign in Eq. (2.8) holds, i.e. if the energy release rate,

$$\mathcal{G} = -\frac{\partial U^e}{B \partial (2a)} = \frac{\partial U_{\text{rel}}^e}{B \partial (2a)} = \frac{\pi a \sigma_{\infty}^2}{8G} (1 + \kappa), \quad (2.10)$$

equals the work of separation (sometimes also called separation energy) per increment of crack area,

$$\frac{\partial U_{\text{sep}}}{B \partial (2a)} = 2\gamma = \Gamma_c, \quad (2.11)$$

which is necessary to create two new crack surfaces (at each crack tip),

$$\mathcal{G}(a) = \Gamma_c. \quad (2.12)$$

This is Griffith's criterion for the onset of unstable crack extension. It balances an “applied” quantity, \mathcal{G} , which depends on the geometry of the structure and the crack as well as external loading with a characteristic material parameter, Γ_c . For $\mathcal{G} < \Gamma_c$, the structure is “safe”, i.e. the crack will not grow. Note that crack extension under linear elastic (brittle) conditions occurs in an unstable manner, always, since different from plastic behaviour there is no other dissipative term in the energy balance.

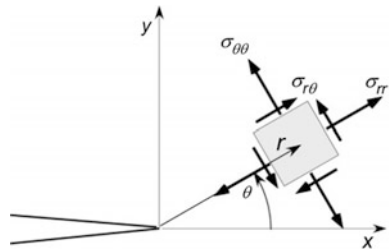
Equation (2.12) yields the macroscopic fracture stress of the centre-cracked panel in plane strain as

$$\sigma_f^{\infty} = \sqrt{\frac{2E'\gamma}{\pi a}}. \quad (2.13)$$

2.2 The Stress-Intensity Approach of Irwin

The stress field at the crack tip is commonly described in dependence on the polar coordinates r , θ , Fig. 2.3.

Fig. 2.3 Cartesian (x , y) and cylindrical (r , θ) coordinates and stresses at the crack tip



Though fundamental solutions of stress fields at singularities in elastic media were published in the early and mid 20th century, already, [16, 35, 38], this knowledge did not find its way into the design of engineering structures. It was Irwin [17] who first realised the essential resemblance of all asymptotic singular stress fields at crack tips and concluded to use the intensities of these fields for fracture mechanics based assessments of structural integrity. Actually, the asymptotic stress fields exhibit a $1/\sqrt{r}$ singularity for all crack opening modes which is governed by a stress intensity factor (SIF). Due to the assumption of linear elastic material behaviour and small deformations, the respective fields of all three modes can be superimposed,

$$\lim_{r \rightarrow 0} \sigma_{ij}(r, \theta) = \frac{1}{\sqrt{2\pi r}} \left[K_I f_{ij}^I(\theta) + K_{II} f_{ij}^{II}(\theta) + K_{III} f_{ij}^{III}(\theta) \right]. \quad (2.14)$$

The subscripts i, j indicate Cartesian or cylindrical coordinates.

- K_I, K_{II}, K_{III} are the SIFs of the three crack opening modes depending on the geometry of the structure and the crack as well as on the external forces.
- $f_{ij}^I, f_{ij}^{II}, f_{ij}^{III}$, are dimensionless angular functions of θ ; the first two are graphically displayed in Fig. 2.4. The distribution of normal stresses, σ_{xx}, σ_{yy} , is symmetric to the ligament, $\theta = 0$, that of shear stresses, σ_{xy} , antisymmetric in mode I; for mode II it is the other way round. Note that the maximum of stresses, σ_{yy} , in opening direction is not in the ligament but at $\pm 60^\circ$.

The associated displacement field is given as

$$u_i(r, \theta) = \frac{1}{2G} \sqrt{\frac{r}{2\pi}} [K_I g_i^I(\theta) + K_{II} g_i^{II}(\theta) + K_{III} g_i^{III}(\theta)], \quad (2.15)$$

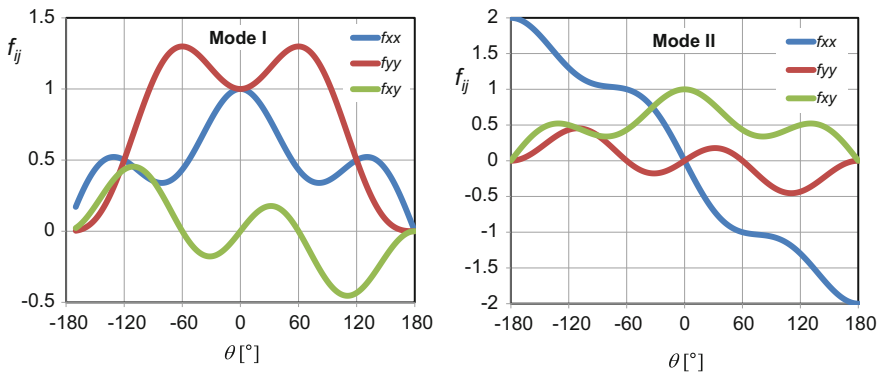


Fig. 2.4 Angular functions of stress fields in Cartesian coordinates at the crack tip in LEFM for mode I and II

Table 2.2 Angular functions of stress and displacement fields in Cartesian coordinates at the crack tip in LEFM

	Mode I	Mode II	Mode III
f_{xx}	$\cos \frac{\theta}{2} (1 - \sin \frac{\theta}{2} \sin \frac{3\theta}{2})$	$-\sin \frac{\theta}{2} (2 - \cos \frac{\theta}{2} \cos \frac{3\theta}{2})$	0
f_{yy}	$\cos \frac{\theta}{2} (1 + \sin \frac{\theta}{2} \sin \frac{3\theta}{2})$	$\sin \frac{\theta}{2} \cos \frac{\theta}{2} \cos \frac{3\theta}{2}$	0
f_{zz}	0 plane stress $2\nu \cos \frac{\theta}{2}$ plane strain	0 plane stress $-2\nu \sin \frac{\theta}{2}$ plane strain	0
f_{xy}	$\sin \frac{\theta}{2} \cos \frac{\theta}{2} \cos \frac{3\theta}{2}$	$\cos \frac{\theta}{2} (1 - \sin \frac{\theta}{2} \sin \frac{3\theta}{2})$	0
f_{xz}	0	0	$-\sin \frac{\theta}{2}$
f_{yz}	0	0	$\cos \frac{\theta}{2}$
g_x	$\cos \frac{\theta}{2} [\kappa - 1 + 2 \sin^2 \frac{\theta}{2}]$	$\sin \frac{\theta}{2} [\kappa + 1 + 2 \cos^2 \frac{\theta}{2}]$	0
g_y	$\sin \frac{\theta}{2} [\kappa + 1 - 2 \cos^2 \frac{\theta}{2}]$	$-\cos \frac{\theta}{2} [\kappa - 1 - 2 \sin^2 \frac{\theta}{2}]$	0
g_z	0 for plane strain	0 for plane strain	$4 \sin \frac{\theta}{2}$

where G is the shear modulus and g_I^I , g_I^{II} , g_I^{III} are respective angular functions again. Displacements are not singular at the crack tip, of course, but vanish for $r \rightarrow 0$.

Table 2.2 summarises all angular functions for the three modes.

Irwin also depicted the relationship between the stress intensity and the energy approach by deriving that

$$\mathcal{G} = \frac{K_I^2}{E'}. \quad (2.16)$$

Corresponding to Griffith's Eq. (2.12), a criterion for unstable “brittle” fracture in LEFM can be established based on the SIF,

$$K_I(a) = K_{Ic}, \quad (2.17)$$

which balances an “applied” quantity, K_I , depending on the geometry of the structure and the crack as well as external loading with a characteristic material parameter, the “fracture toughness”, K_{Ic} . For $K_I < K_{Ic}$, the structure is “safe”, i.e. the crack will not grow. The fracture toughness has to be experimentally determined according to standards like ASTM E399 [4]. For further details see Sect. 7.2.2 on linear-elastic plane-strain fracture toughness.

More generally, the energy release rate in mixed mode results from the SIFs by

$$\mathcal{G} = \mathcal{G}_I + \mathcal{G}_{II} + \mathcal{G}_{III} = \frac{K_I^2}{E'} + \frac{K_{II}^2}{E'} + \frac{K_{III}^2}{2G}. \quad (2.18)$$

Together with Eq. (2.12), this relation suggests a simple fracture criterion for mixed mode [14, 15], which is not always confirmed by experiments, however. Other criteria have been proposed by Erdogan and Sih [9], Sih [34] or Richard and Kuna [31], for instance. An extensive literature exists on mixed mode problems which are still a matter of research. Further details would overshoot the purpose of the present book.

Likewise, any up-to-date overview on fatigue crack growth would exceed the self-established limits and this issue is solely mentioned to demonstrate the wide application range of the K -concept. Paris and Erdogan [26] correlated the rate of crack extension, da/dN , where N is the number of loading cycles, with the cyclic stress intensity factor, $\Delta K = K_{\max} - K_{\min}$, and found a power law relationship

$$\frac{da}{dN} \sim \Delta K^n, \quad (2.19)$$

where the exponent, n , for many metallic materials is typically between 2 and 4. Enhancements of this “Paris-equation” include effects of the mean stress, crack closure effects etc.

A final remark appears necessary on so-called “higher-order” approaches. For simplicity and because the singular terms of the stress fields, Eq. (2.14), appeared to be dominant, Irwin and his successors restricted to the SIFs (or the energy release rate, \mathcal{G}) as crack driving forces. Irwin, however, was aware that the asymptotic stress field included a second non-vanishing parameter for $r \rightarrow 0$: *“The influence of the test configuration, loads and crack length upon the stresses near an end of the crack may be expressed in terms of two parameters. One of these is an adjustable uniform stress parallel to the direction of a crack extension.... The other parameter, called the stress intensity factor, is proportional to the square root of the force tending to cause crack extension”*. Williams [39] presented a series expansion of the stress field for the biaxially loaded Griffith crack, in which

$$\sigma_{xx} = \frac{A_{-1}}{\sqrt{r}} \cos \frac{\theta}{2} \left(1 - \sin \frac{\theta}{2} \sin \frac{3\theta}{2} \right) - \frac{C_{-1}}{\sqrt{r}} \sin \frac{\theta}{2} \left(2 + \cos \frac{\theta}{2} \cos \frac{3\theta}{2} \right) + A_0 \quad (2.20)$$

contains a constant stress

$$A_0 = \frac{1}{2} \sigma_{\infty} (\lambda - 1). \quad (2.21)$$

depending on the biaxiality factor, λ , for the Griffith crack and more generally on the specimen geometry. This issue of a second parameter in fracture mechanics became topical many years later in discussions on “geometry effects” on the fracture toughness, see historical overview by Brocks and Schwalbe [7], leading Rice [30] to come up with the T -stress approach,

$$\sigma_{ij}(r, \theta) = \frac{K_I}{\sqrt{2\pi r}} f_{ij}(\theta) + T \delta_{1i} \delta_{1j}. \quad (2.22)$$

Understanding the effect of the T -stress requires the investigation of plastic zones at the crack tip and will be discussed in Chap. 4 on extension of LEFM for small-scale yielding.

2.3 Determination of SIFs

Stress intensity factors have attained an important role in the assessment of engineering structures against brittle fracture. They are a measure of the “powerfulness” of the $1/\sqrt{r}$ -singularity of stresses,

$$\begin{Bmatrix} K_I \\ K_{II} \\ K_{III} \end{Bmatrix} = \lim_{r \rightarrow 0} \sqrt{2\pi r} \begin{Bmatrix} \sigma_{yy}(r, \theta = 0) \\ \sigma_{xy}(r, \theta = 0) \\ \sigma_{yz}(r, \theta = 0) \end{Bmatrix}. \quad (2.23)$$

Correspondingly,

$$\begin{Bmatrix} K_I \\ K_{II} \\ K_{III} \end{Bmatrix} = \lim_{r \rightarrow 0} \sqrt{\frac{2\pi}{r}} \begin{Bmatrix} \frac{1}{\kappa+2} u_y(r, \theta = \pi) \\ \frac{1}{\kappa+1} u_x(r, \theta = \pi) \\ \frac{1}{4} u_z(r, \theta = \pi) \end{Bmatrix} \quad (2.24)$$

holds for the crack edge displacements. From Eq. (2.23), the dimension of K can be read as [force \times length $^{-3/2}$]. Typical units are $\text{MPa}\sqrt{\text{m}} = 10\sqrt{10} \text{ N mm}^{-3/2}$.

If the asymptotic stress fields, $\sigma_{ij}(r, \theta)$, or the crack edge displacements are known from analytical or numerical solutions, the associated K -factors can be immediately calculated by comparisons with Eqs. (2.23) or (2.24). Calculations based on the displacements require an assumption on plane stress or plane strain

Table 2.3 SIFs for some basic loading cases

(a) Griffith crack	K_I	K_{II}	K_{III}
Uniaxial tension, σ_{yy}^∞	$\sigma_{yy}^\infty \sqrt{\pi a}$	0	0
In-plane shear, $\sigma_{yx}^\infty = \sigma_{xy}^\infty$	0	$\sigma_{xy}^\infty \sqrt{\pi a}$	0
Anti-plane shear, σ_{yz}^∞	0	0	$\sigma_{yz}^\infty \sqrt{\pi a}$
Crack face pressure, p_0	$p_0 \sqrt{\pi a}$	0	0
Two pin-forces, F , wedging problem	$\frac{F}{\pi B a} \sqrt{\pi a}$	0	0
(b) circular crack	K_I	K_{II}	K_{III}
Uniaxial tension, σ_{yy}^∞	$\sigma_{yy}^\infty \frac{2}{\pi} \sqrt{\pi a}$	0	0
Crack face pressure, p_0	$p_0 \frac{2}{\pi} \sqrt{\pi a}$	0	0

conditions, neither of which is actually realised in a real three-dimensional structure. It is hence approximately assumed, frequently, that the free surface of a specimen is in plane stress and its mid section in plane strain.

SIFs depend on the geometry of the structure, the type of loading (tension or bending, for instance), the crack configuration and (linearly) on the external forces. K -factors of some elementary loading cases of the Griffith crack and a circular (“penny-shaped”) centre crack of radius a in an “infinite cylinder [36] are listed in Table 2.3.

The SIF of an arbitrary plane crack problem can be written as a generalisation of the expressions in Table 2.3,

$$K = \sigma_{\infty} \sqrt{\pi a} Y(a/W, \dots), \quad (2.25)$$

where σ_{∞} is an appropriately defined “nominal stress” in the far-field of the crack and Y a dimensionless function of geometry parameters like a/W , which can be determined from analytical or numerical solutions. Classical handbooks like

- “Compendium of Stress Intensity Factors”, Rooke and Cartwright [32],
- “The Stress Analysis of Cracks Handbook”, Tada et al. [37],
- “Stress Intensity Factors Handbook”, Murakami et al. [23]

provide numerous solutions and respective fit functions. It is subject to the engineers’ experience with modelling to attribute real structures to these compilations of problems and approximate solutions. The principle of superposition supplies a universal methodology to generate geometry functions of complex structures and loading cases from fundamental solutions. Due to the linear-elastic constitutive equations and the assumption of small deformations, the boundary value problem is linear so that K -factors of the same mode may be added,

$$K_{\alpha} = \sum_n K_{\alpha}^{(n)}, \quad \alpha = \text{I, II, III}, \quad n = \text{loading cases} \quad (2.26)$$

For instance, the mode I and II SIFs of an infinite panel with a centre crack of length $2a$ which is inclined by an angle, β , to the x -axis under tensile and shear stresses, σ_{∞} , τ_{∞} , are obtained by superposition from equations given in Table 2.3 as

$$\begin{aligned} K_{\text{I}} &= (\sigma_{\infty} \sin \beta - \tau_{\infty} \cos \beta) \sin \beta \sqrt{\pi a} \\ K_{\text{II}} &= (\sigma_{\infty} \cos \beta + \tau_{\infty} \sin \beta) \sin \beta \sqrt{\pi a}. \end{aligned} \quad (2.27)$$

SIFs for test specimens which are used to determine fracture parameters like K_{Ic} , Eq. (2.17), can be found in ASTM E399 [4], see Sect. 7.2.2.

The calculation of SIFs for real structures and practically relevant loading cases requires complex mathematical methods. In the past, analytical solutions have been obtained by complex stress functions [24], series expansions [39] or integral

transforms [36]. They do not necessitate complete solutions of the boundary value problem but just the stress field at the crack tip. Stress fields without the characteristic $1/\sqrt{r}$ singularity do not affect the SIF. If numerical solutions of stress or displacement fields are available, K -factors can be determined with Eqs. (2.23) or (2.24).

With the emerging power of soft- and hardware numerical methods like boundary element or finite element methods, e.g. [21], became increasingly important and popular also for the determination of K -factors. Respective analyses can be done for 3D configurations with straight or curved crack fronts, when the stress field and the SIF depend on the crack-front coordinate, z , or an arc length, s_c , respectively, $K(z)$ or $K(s_c)$, see example of a railway axle in Sect. 7.1.3. In the beginning, numerically calculated courses of stresses or displacements were extrapolated to calculate SIFs according to Eqs. (2.23) and (2.24), but this did not yield sufficiently accurate results, particularly if they are based on stresses. More advanced methods exploit the relation to the energy release rate, Eqs. (2.16) and (2.18) where the latter is commonly evaluated by a domain integral [1], which was first suggested by Parks [27, 28] and became an established technique in FEM [33]. More details will be presented in Sect. 7.1.2 on the numerical determination of energy release rate and J -integral and Sect. 7.1.3 on the numerical determination of SIFs.

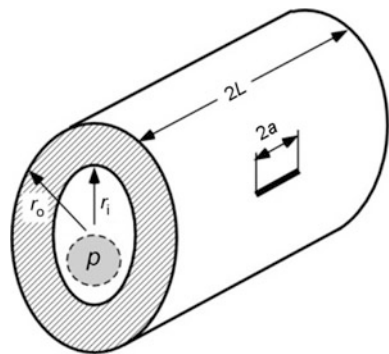
2.3.1 Cracked Cylinders

An axial through-crack of length $2a$ in a long pressurised cylinder or pipe, Fig. 2.5, can be considered as a Griffith crack ($W \Rightarrow L$), as the condition of $a/L \ll 1$ is fulfilled. The remote stresses result from the well-known formula

$$\sigma_{\infty} = \sigma_t = p \frac{r_i}{t} \quad (2.28)$$

for circumferential (tangential) stresses, $\sigma_t = \sigma_{\varphi\varphi}$, in a thin walled cylinder, $t/r_o \ll 1$, where r_i and $t = r_o - r_i$ are the (inner) radius and the wall-thickness,

Fig. 2.5 Thick-walled cylinder of length, $2L$, under internal pressure, p , with axial through-crack, $2a$, inner radius r_i , outer radius r_o , Young's modulus E , Poisson's ratio ν



respectively, of the tube and p is the internal pressure. A cylinder is not plane as a panel, however, but bent. Thus, the geometry function depends on the curvature and the wall thickness, $Y(a/\sqrt{r_i t})$. In the following, the shell parameter $\lambda_s = a/\sqrt{r_i t}$ is introduced. As the stress intensity in a cylindrical tube was first analysed by Folias [10], this function is addressed as Folias factor in the literature, e.g. Kiefner et al. [20]. Misleadingly, it is sometimes associated with bulging of the cylinder wall in the vicinity of the crack (BS 7910, [8]).

Murakami et al. [23] present diagrams and tables of $Y(\lambda_s)$ in the range $0 \leq \lambda_s \leq 4.4$, and British Standard 7910 tabulated values for $0 \leq \lambda_s \leq 6.7$ and $5 \leq r_o/t \leq 100$. In his solution of the boundary value problem, Folias [10] derived

$$\frac{\sigma_{\text{shell}}}{\sigma_{\text{panel}}} = Y(\lambda_s) \approx 1 + (c_1 + c_2 \ln \lambda_s) \lambda_s^2 + \mathcal{O}\left(\frac{1}{r_o^2}\right), \quad (2.29)$$

which represents a good approximations of the tabulated values of BS 7910 [8] for $\lambda_s = a/\sqrt{r_o t} \leq 6.5$, taking $c_1 = 0.4612$, $c_2 = -0.1806$.

Equation (2.28) holds approximately for thin-walled cylinders, $t/r_o \ll 1$, only. Stresses in thick-walled cylinders (without any crack) can be derived from the axisymmetric boundary value problem in cylindrical coordinates (r, φ, z) , $\partial(\cdot)/\partial\varphi = 0$, described by the balance equations,

$$\frac{\partial\sigma_{rr}}{\partial r} + \frac{1}{r}(\sigma_{rr} - \sigma_{\varphi\varphi}) = 0, \quad \frac{\partial\sigma_{zz}}{\partial z} = 0, \quad (2.30)$$

and Hooke's law, Eq. (2.1), together with the boundary conditions $\sigma_{rr}(r_o) = 0$, $\sigma_{rr}(r_i) = -p$. The equivalence condition for axial forces in a capped cylinder,

$$N_z = 2\pi \int_{r_i}^{r_o} \sigma_{zz} r dr = \pi \int_{r_i}^{r_o} (\sigma_{rr} + \sigma_{\varphi\varphi}) r dr = \pi r_i^2 p, \quad (2.31)$$

results in

$$\sigma_{zz} = 1/2(\sigma_{rr} + \sigma_{\varphi\varphi}). \quad (2.32)$$

Finally, Lamé's equations, are obtained,

$$\begin{aligned} \sigma_{rr} &= \frac{r_i^2}{r_o^2 - r_i^2} \left[1 - \left(\frac{r_o}{r}\right)^2 \right] p \leq 0, \\ \sigma_t &= \sigma_{\varphi\varphi} = \frac{r_i^2}{r_o^2 - r_i^2} \left[1 + \left(\frac{r_o}{r}\right)^2 \right] p, \\ \sigma_{zz} &= \frac{r_i^2}{r_o^2 - r_i^2} p \end{aligned} \quad (2.33)$$

which are graphically displayed in Fig. 2.6. Maximum circumferential stresses occur at the inner surface.

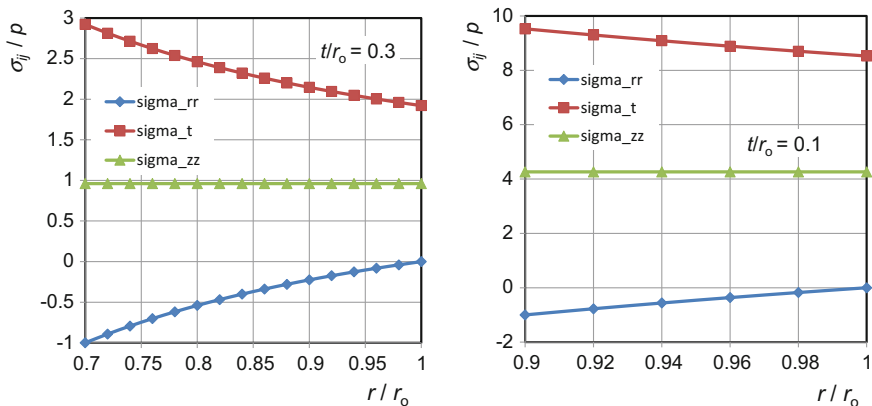


Fig. 2.6 Radial, circumferential (tangential) and axial stresses, σ_{rr} , $\sigma_t \equiv \sigma_{\phi\phi}$, σ_{zz} , in an uncracked thick-walled cylinder, $t/r_o = 0.3$ and 0.1 , under internal pressure, p

2.3.2 Semi-elliptical Surface Crack

Cracks originating from the surface of a component without penetrating the whole wall thickness are of great practical relevance. They may initiate from notches or surface roughness under cyclic loading, thermal stresses or corrosion and grow under service loads to a critical size when failure of the structure occurs. A simplified model for the variety of crack shapes is the semi-elliptical surface flaw, see Fig. 2.7, which is characterised by its depth a , the small principal axis, and its length $2c$, twice the large principal axis, with the aspect ratio,

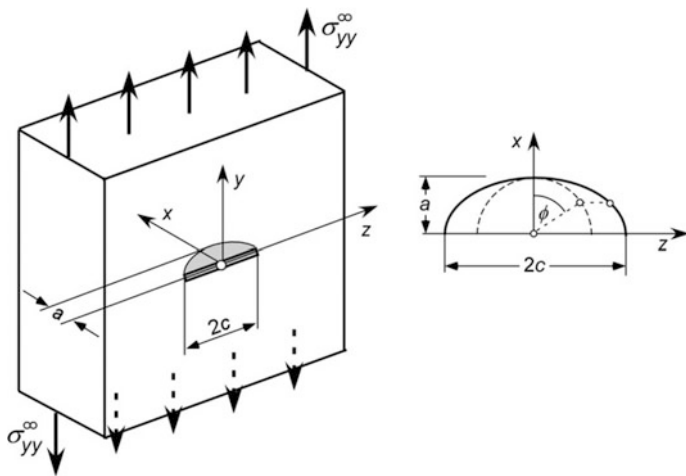


Fig. 2.7 PS(T) specimen (ASTM E1823 [5]) with semi-elliptical surface crack

$$0 \leq k = a/c \leq 1. \quad (2.34)$$

An arbitrary point on the crack front may be identified by a parametric angle, ϕ , which is defined by the projection of an ellipse point to a circle of radius a . The deepest point of the crack in the centre is characterised by $\phi = 0$, and the penetrations points of the crack front with the surface by $\phi = \pm\pi/2$. Irwin [18] presented the solution for an elliptical inner crack under uniaxial tension

$$K_I(\phi) = \sigma_\infty \sqrt{\pi a} \frac{f_\phi(\phi)}{E(k)}, \quad (2.35)$$

with the elliptical shape function,

$$f_\phi(\phi) = (\cos^2 \phi + k^2 \sin^2 \phi)^{1/4}, \quad (2.36)$$

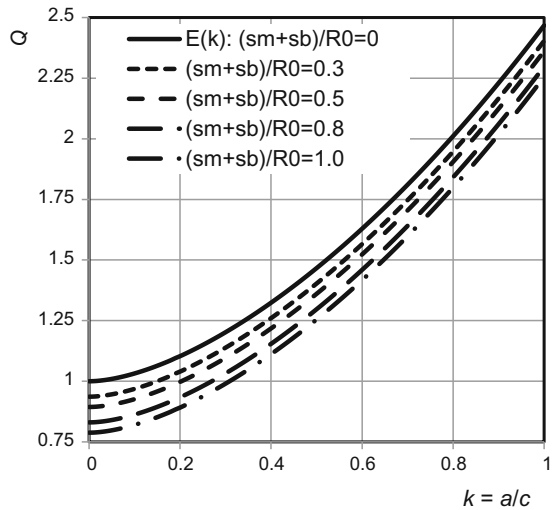
which becomes $f_\phi = 1$ for the penny-shaped crack ($k = 1$), and the 2nd kind elliptical integral,

$$E(k) = \int_0^{\pi/2} \sqrt{1 - (1 - k^2) \sin^2 \phi} d\phi, \quad (2.37)$$

which becomes $E(k) = 1$ for the Griffith crack ($2c \rightarrow \infty$, $k = 0$) and $E(k) = \pi/2$ for the penny-shaped crack ($k = 1$), see Fig. 2.8. The extrema of $K_I(\phi)$ are

$$\begin{aligned} K_I^{\max} &= K_I(0) = \frac{\sigma_\infty \sqrt{\pi a}}{E(k)} \\ K_I^{\min} &= K_I(\pm \frac{\pi}{2}) = \frac{\sigma_\infty \sqrt{\pi a \sqrt{k}}}{E(k)}. \end{aligned} \quad (2.38)$$

Fig. 2.8 Shape factor of semi-elliptical surface flaws: 2nd kind elliptical integral $E(k)$ and SSY modifications, Eq. (4.10), according to ASME BPVC



Analogous to Eq. (2.25), arbitrary structures with semi-elliptical surface cracks are described by geometry functions, $h_j(\phi)$, which have been calculated numerically and can be found in the literature, for instance Heliot et al. [13], Isida et al. [19], McGowan and Raymund [22], Newman and Raju [25], Raju and Newman [29] among others. General inhomogeneous stress fields are captured by superposition. The problem of a semi-elliptical surface crack in an arbitrary tensile stress field is thus treated as a crack with pressure, $\bar{p}(x)$, on the crack faces which equals the nominal stress distribution in the uncracked component at the position of the crack, $\sigma_{yy}^0(x)$, and the latter is fitted by a polynomial,

$$\sigma_{yy}^0(x) = \sum_j \sigma_j^0 \left(\frac{x}{t}\right)^j. \quad (2.39)$$

For $j = 0$ the part of homogeneous tension is obtained, for $j = 1$ pure bending, etc. The resulting stress intensity factor is

$$K_I(\phi) = \sum_j \sigma_j^0 \sqrt{\pi a} \frac{f_\phi(\phi)}{E(k)} h_j(\phi). \quad (2.40)$$

In the following, a surface crack in a pressure vessel is considered. According to Eq. (2.33), $\sigma_{\varphi\varphi}(r)$ in the uncracked cylinder is maximum at the inner surface, $r = r_i$, and hence a crack at the inner surface is most hazardous. According to Eq. (2.39), $\sigma_{yy}^0(x) = \sigma_{\varphi\varphi}(r - r_i)$ is expanded in a series. The ASME Boiler and Pressure Vessel Code [3] suggests a linear fit, namely a constant fraction, the membrane stresses, σ_m , and the bending stresses, σ_b ,

$$\sigma_{\varphi\varphi}(x) = (\sigma_m + \sigma_b) - 2\sigma_b \left(\frac{x}{t}\right), \quad (2.41)$$

with

$$\begin{aligned} \sigma_m &= p_0 \left[1 - \frac{r_o^2}{2(r_o^2 + r_i^2)} \left(1 - \frac{r_i^2}{(r_i + a)^2} \right) \frac{t}{a} \right], \\ \sigma_b &= p_0 \frac{r_o^2}{2(r_o^2 + r_i^2)} \left(1 - \frac{r_i^2}{(r_i + a)^2} \right) \frac{t}{a} \end{aligned} \quad (2.42)$$

and $p_0 = p \frac{r_o^2 - r_i^2}{r_o^2 + r_i^2}$ as abbreviation. The SIF is

$$K_I(\phi) = \left[\sigma_m h_0(\phi) + \sigma_b \left(h_0(\phi) - 2 \frac{a}{t} h_1(\phi) \right) \right] \sqrt{\pi a} \frac{f_\phi(\phi)}{E(k)}. \quad (2.43)$$

Considering its maximum at $\phi = 0$ and the condition for brittle fracture, Eq. (2.17),

$$K_I^{\max} = (M_m \sigma_m + M_b \sigma_b) \frac{\sqrt{\pi a}}{E(k)} \leq K_{Ic}, \quad (2.44)$$

the critical pressure, p_c , for an assumed or detected crack depth, a , or a critical crack depth, a_c , for the service pressure can be determined accounting for an additional safety factor. The coefficients $M_m = h_0(0)$ and $M_b = h_0(0) - 2(a/t)h_1(0)$ for membrane and bending stresses can be found in the ASME BPVC [3], which also introduces a modified shape factor, Q , instead of $E(k)$ accounting for small plastic zones at the crack tip, see Sect. 4.1 on the equivalent elastic crack.

ASTM E2899 [6] defines test methods and nomenclature for surface cracks under tension and bending. Recent applications can be found in Arafah et al. [2].

References

1. Abaqus (2014) User's manual, Version 6.12. Dassault Systèmes Simulia Corp, Providence, RI, USA
2. Arafah D, Madia M, Zerbst U, Beretta S, Cristea ME (2015) Instability analysis of pressurized pipes with longitudinal surface cracks. *Int J Press Vessels Pip* 126–127:48–57
3. ASME BPVC (2015) Boiler and pressure vessel code. The American Society of Mechanical Engineers
4. ASTM E399 (2012) Standard test method for linear-elastic plane-strain fracture toughness K_{Ic} of metallic materials. *Annual Book of ASTM Standards*, vol 03.01, American Society for Testing and Materials, West Conshohocken (PA), USA
5. ASTM E1823 (2013) Standard Terminology Relating to Fatigue and Fracture Testing. *Annual Book of ASTM Standards*, vol 03.01, American Society for Testing and Materials, West Conshohocken (PA), USA
6. ASTM E2899 (2015) Standard test method for measurement of initiation toughness in surface cracks under tension and bending. *Annual Book of ASTM Standards*, vol 03.01, American Society for Testing and Materials, West Conshohocken (PA), USA
7. Brocks W, Schwalbe KH (2015) Experimental and numerical fracture mechanics—an individually dyed history. In: Hütter G, Zybelle L (eds) *Recent trends in fracture and damage mechanics*. Springer, Heidelberg, pp 23–57
8. BS 7910 (2005) Guide to methods for assessing the acceptability of flaws in metallic structures, British Standards
9. Erdogan F, Sih GE (1963) On the crack extension in shells and plates under plane loading and transverse shear. *J Basic Eng* 85:527–529
10. Folias ES (1965) An axial crack in a pressurized cylindrical shell. *Int J Fract Mech* 1:104–113
11. Griffith AA (1920) The phenomena of rupture and flow in solids. *Phil Trans Roy Soc London A* 211:163–198
12. Griffith AA (1924) Theory of rupture. In: Biezeno B, Burgers JM (eds) *Proceedings 1st International Congress for Applied Mechanics*. Waltman Uitgeverij, Delft, pp 55–63
13. Heliot J, Labbens RC, Pelissier-Tanon A (1978) Semi-elliptical cracks in a cylinder subjected to stress gradients. In: Smith CW (ed) *Proceedings of 11th National Symposium on Fracture Mechanics*, ASTM STP, vol 677, pp 341–364
14. Hussain MA, Pu SI, Underwood J (1974) Strain energy release rate for a crack under combined Mode I and Mode II. *ASTM STP* 560:2–28
15. Ichikawa M, Tanaka S (1982) A critical analysis of the relationship between the energy release rate and the stress intensity factors under combined mode loading. *Int J Fract* 18:19–28

16. Inglis CE (1913) Stresses in a plate due to the presence of cracks and sharp corners. *Trans Inst Naval Arch* 60:219–230
17. Irwin GR (1957) Analysis of stresses and strains near the end of a crack traversing a plate. *J Appl Mech* 24:361–364
18. Irwin GR (1962) Crack extension force for a part-through crack in a plate. *Trans ASME, Series E, J Appl Mech* 29:615–634
19. Isida M, Noguchi H, Yoshida T (1984) Tension and bending of finite thickness plates with a semi-elliptical surface crack. *Int J Fract* 26:157–188
20. Kiefner JF, Maxey WA, Eiber RJ, Duffy AR (1973) Failure stress levels of flaws in pressurized cylinders. In: *Progress in flaw growth and fracture toughness testing*. ASTM STP 536:461–481
21. Kuna M (2013) *Finite elements in fracture mechanics*. Springer, Dordrecht
22. McGowan JJ, Raymund M (1978) Stress intensity factor solutions for internal longitudinal semi-elliptical surface flaws in a cylinder under arbitrary loadings. In: Smith CW (ed) *Proceedings of 11th National Symposium Fracture Mechanics*, ASTM STP, vol 677, pp 365–3680
23. Muarakami Y (ed) (1987) *Stress intensity factors handbook*, 3rd edn. Pergamon, New York
24. Muskhelishvili NI (1977) *Some basic problems of the mathematical theory of elasticity*. Springer, Dordrecht
25. Newman JN, Raju IS (1981) An empirical stress-intensity-factor equation for the surface crack. *J Eng Fract Mech* 15:185–192
26. Paris PC, Erdogan F (1963) A critical analysis of crack propagation laws. *J Basic Eng Trans Am Soc Mech Eng D85*:528–534
27. Parks DM (1974) A stiffness derivative finite element technique for determination of crack tip stress intensity factors. *Int J Fract* 10:487–502
28. Parks DM (1977) The virtual crack extension method for nonlinear material behavior. *Comput Meth Appl Mech Eng* 12:353–364
29. Raju IS, Newman JN (1979) Stress-intensity-factors for a wide range of semi-elliptical surface cracks in finite thickness plates. *J Eng Fract Mech* 11:817–829
30. Rice JR (1974) Limitations to the small scale yielding approximation for crack tip plasticity. *J Mech Phys Solids* 17–26
31. Richard HA, Kuna M (1990) Theoretical and experimental study of superimposed fracture modes I, II, III. *Eng Fract Mech* 35:949–960
32. Rooke DP, Cartwright DP (1976) *Compendium of stress intensity factors*. Stationary Office, GB
33. Shih CF, Moran B, Nakamura T (1986) Energy release rate along a three-dimensional crack front in a thermally stressed body. *Int J Fracture* 30:79–102
34. Sih GE (1974) Strain energy density factor applied to mixed mode crack problems. *Int J Fracture* 10:305–321
35. Sneddon IN (1946) The distribution of stress in the neighbourhood of a crack in an elastic solid. *Proc Roy Soc A187*:229–260
36. Sneddon IN (1973): Integral transform methods—circular cracks. In: Shih GC (ed) *Mechanics of fracture*, vol 1. *Methods of analysis and solution of crack problems*, pp 350–363
37. Tada H, Paris PC, Irwin GR (2000) *The stress analysis of cracks handbook*, 3rd edn. ASME, doi:[10.1115/1.801535](https://doi.org/10.1115/1.801535)
38. Westergaard HM (1939) Bearing pressures und cracks. *J Appl Mech* 6:49–53
39. Williams ML (1957) On the stress distribution at the base of a stationary crack. *J Appl Mech* 24:109–114



<http://www.springer.com/978-3-319-62751-9>

Plasticity and Fracture

Brocks, W.

2018, XVIII, 173 p. 75 illus., Hardcover

ISBN: 978-3-319-62751-9